DRFC-CAD EUR-CEA-FC-15

CONFINEMENT MARGINS FOR IGNITION AND DRIVEN OPERATION IN ITER EDA ID

J. JOHNER

September 1995

CONFINEMENT MARGINS FOR IGNITION AND DRIVEN OPERATION IN ITER EDA ID

J. JOHNER

September 1995

ASSOCIATION EURATOM-CEA SUR LA FUSION
Département de Recherches sur la Fusion Contrôlée
Centre d'Etudes Nucléaires de Cadarache
13108 SAINT-PAUL-LEZ-DURANCE CEDEX (FRANCE)

Abstract

Preliminary calculations for ITER EDA ID have been performed using the 1/2D thermal equilibrium code HELIOS. It is found that:

- The maximum ignition margin for ITER ID (29%) is 6% less than for ITER OD (35%) and 5% less than for ITER CDA (34%).

- Decreasing the ratio τ^*_{He}/τ_E from the nominal value 10 to a value of 5 gives a 12% gain in the maximum ignition margin. Increasing the ratio from 10 to 15 causes a 22% loss in the margin. Furthermore, ignited equilibria no longer exist for $\tau^*_{He}/\tau_E \geq 17.6$.

- Operation in driven mode with 50 MW of external power increases the confinement capability by 13%. With 100 MW, the improvement is 24%.

- Lowering the fusion power from 1500 to 1000 MW slightly improves the maximum ignition margin (+5%) and allows operation below the Greenwald density limit.

- A 10% reduction of the toroidal magnetic field with a correlative diminution of the plasma current for constant safety factor operation, causes a dramatic reduction (-18%) of the maximum ignition margin.

- A fraction of neon of 0.68% would completely suppress the ignition margin. Furthermore, ignited equilibria, with the nominal fusion power and τ^*_{He}/τ_E, no longer exist when the neon fraction exceeds 0.75%.

1 Introduction

Results of 1/2D calculations performed with the HELIOS code [1] are presented using the following approximations and assumptions:

- No plasma volume correction due to the lower X-point,
- No synchrotron radiation,
- The confinement time for operation in H-mode with grassy ELMs is taken to be

$$\tau_{E_{\text{scaling}}} = 0.85 \times \tau_{E_{\text{ITERH-93P-ELMfree}}}$$

with [2]

$$\tau_{E_{\text{ITERH-93P-ELMfree}}} = 3.6 \times 10^{-7.57} \frac{M_{eff}^{0.41}\, \kappa_X^{0.66}\, I_p^{1.06}\, (\overline{n})^{0.17}\, B_t^{0.32}\, R^{1.9}\, a^{-0.11}}{P_{net}^{0.67}} \quad \text{(MKSA)}$$

where the effective atomic mass M_{eff} is taken to be M_{eff}=2.5 and P_{net} is defined as

$$P_{net} = P_\alpha + P_{OH} + P_{ext} - P_{rad}$$

where P_α, P_{OH}, P_{ext}, and P_{rad} are the alpha power coupled to the plasma, the ohmic power, the external power, and the radiation losses (bremsstrahlung), respectively.

2 ITER parameters and model assumptions

The following parameters are taken for ITER CDA, ITER OD and ITER ID:

- ITER CDA

$$R = 6.00\ \text{m},\ \ a = 2.15\ \text{m},\ \ I_p = 22\ \text{MA},$$

$$B_t(R) = 4.85\ \text{T} \quad \text{giving} \quad q_{\psi 95} \simeq 3.01,$$

$$\kappa_{95} = 1.98,\ \ \kappa_X = 2.22,\ \ \delta_{95} = 0.39,\ \ \delta_X = 0.58$$

$$P_{fus} = 1100\ \text{MW}$$

The volume correction due to the symmetrical X-points is taken into account.

- ITER OD

$$R = 8.11\ \text{m},\ \ a = 3\ \text{m},\ \ I_p = 24\ \text{MA},$$

$$B_t(R) = 5.72\ \text{T} \quad \text{giving} \quad q_{\psi 95} \simeq 3.02,$$

$$\kappa_{95} = 1.55,\ \ \kappa_X = 1.60,\ \ \delta_{95} = \delta_X = 0.25$$

$$P_{fus} = 1500\ \text{MW}$$

- ITER ID

$$R = 8.14\ \text{m},\ \ a = 2.80\ \text{m},\ \ I_p = 21\ \text{MA},$$

$$B_t(R) = 5.68\ \text{T} \quad \text{giving} \quad q_{\psi 95} \simeq 3.02,$$

$$\kappa_{95} = 1.60,\ \ \kappa_X = 1.75,\ \ \delta_{95} = \delta_X = 0.24$$

$$P_{fus} = 1500\ \text{MW}$$

The volume correction due to the lower X-point is not taken into account.

Following the recommendations of the JCT and Home Team members, we take

$$f_{Be} = \frac{n_{Be}}{n} = 2\ \%$$

where n_{Be} is the beryllium density and n the electron density. f_{Be} will be denoted the beryllium fraction.

Following the same recommendations, we take

$$n(\rho) = n_0(1-\rho^2)^{\alpha_n} \qquad \text{with} \qquad \alpha_n = 0.15 \tag{1}$$

The recommended temperature profile is:

$$T(\rho) = T_0(1-\rho^4)^3 \tag{2}$$

The corresponding peaking factor is

$$\frac{T_0}{\langle T\rangle} = \frac{35}{16} = 2.1875$$

The present version of the HELIOS code only accepts temperature profiles of the form:

$$T(\rho) = T_0(1-\rho^2)^{\alpha_T} \tag{3}$$

The value of α_T giving the same temperature peaking factor is:

$$\alpha_T = \frac{19}{16} = 1.1875$$

The above values for α_n and α_T will be taken for all the following calculations.

We have represented in Fig. 1 the density profile given by Eq. (1) (dashed line) and the temperature profiles given by Eq. (2) (solid line) and Eq. (3) (dash-dot line). All the profiles are normalized to the volume averaged values.

3 POPCON plot for constant P_{fus}, P_{ext} and τ^*_{He}/τ_E

We consider a tokamak with given density and temperature profiles and a given beryllium fraction.

Choosing a value of the temperature $\langle T\rangle_n$ (density averaged temperature) and of the helium fraction f_{He}, we can calculate the density $\langle n\rangle$ corresponding to a given total fusion power P_{fus} from the following equation

$$P_{fus}(\langle n\rangle, \langle T\rangle_n) = C_\alpha \frac{\langle n\rangle^2}{4} \overline{\sigma v}^*_{DT}(\langle T\rangle_n)\,(E_\alpha + E_n)\ V$$

where $\overline{\sigma v}^*_{DT}(\langle T\rangle_n)$ is the profile averaged thermonuclear reaction rate and where the dilution coefficient C_α takes account of He and Be fractions [1].

- The helium particle content N_{He} and the helium source S_{He} may now be deduced, giving the apparent helium confinement time

$$\tau^*_{He} = \frac{N_{He}}{S_{He}}$$

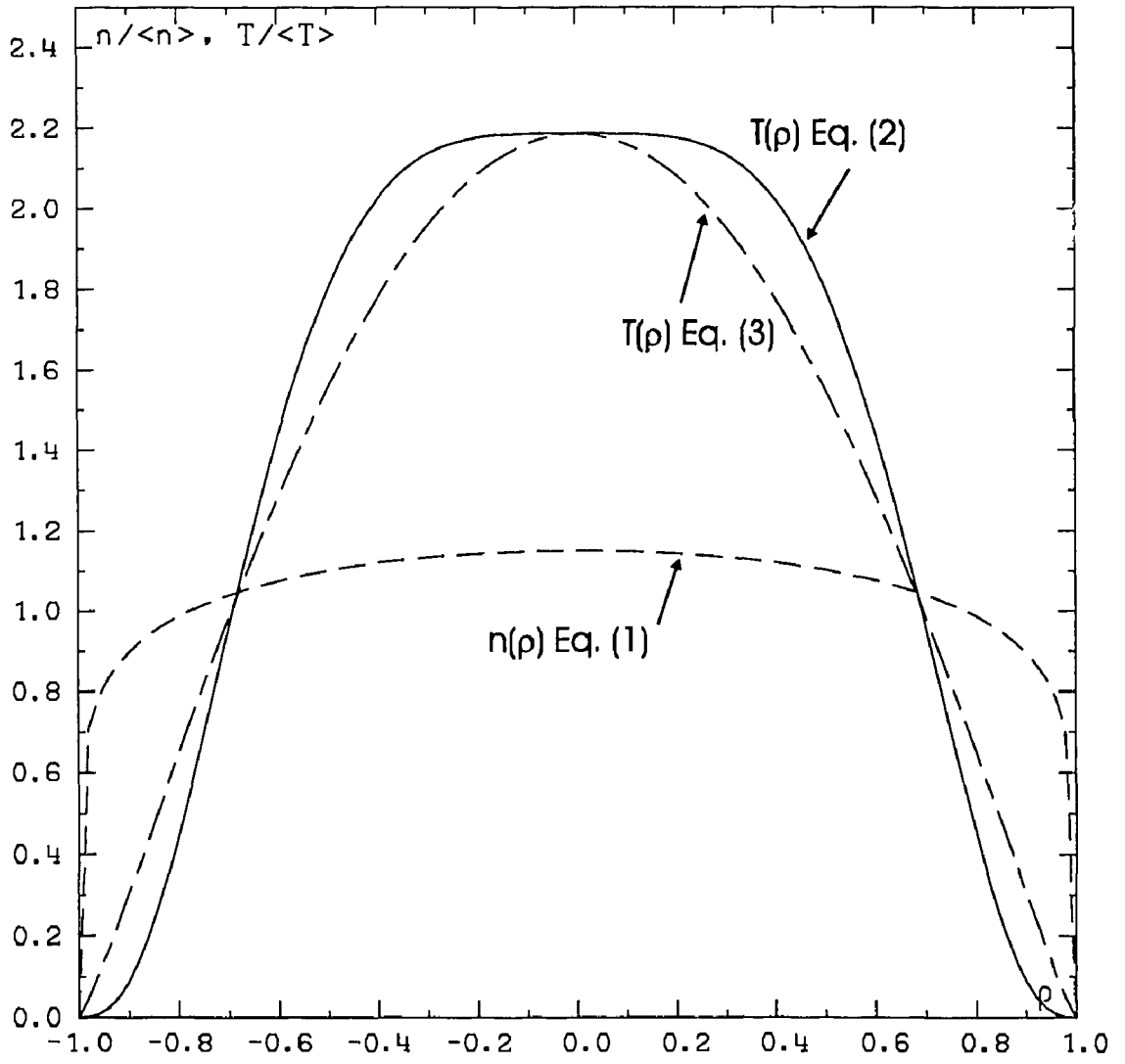

Figure 1: Density and temperature profiles.

- The alpha, ohmic sources and radiation losses may be computed as well as the thermal energy content. For a given external power P_{ext}, the thermal equilibrium equation

$$P_\alpha + P_{OH} + P_{ext} = P_{rad} + \frac{W_{th}}{\tau_E}$$

yields the required energy confinement time τ_E.

Imposing a constraint on τ^*_{He}/τ_E gives an equation for f_{He} which has two or zero solutions. The corresponding curve in the $(\langle n \rangle, \langle T \rangle_n)$ plane is a closed curve.

For each point lying on the above curve, the confinement time given by the scaling law may be computed, leading to the confinement capability M defined as

$$M = \frac{\tau_{E\text{scaling}}}{\tau_E}$$

where τ_E is the **required** energy confinement time given by the thermal equilibrium equation.

The confinement margin ΔM is defined as $\Delta M = M - 1$. It will always be expressed in percent.

4 Comparison between ITER CDA, ITER OD and ITER ID

4.1 ITER ID versus ITER OD

Choosing P_{fus}=1500 MW, τ^*_{He}/τ_E=10, the POPCON plot for ignition (P_{ext}=0) is represented in Fig. 2 for ITER OD (dashed line) and ITER ID (solid line). The confinement capabilities are also given. The upper part of the closed curve corresponds to values of the confinement capability which are in general below 1. The corresponding value of β_N (the normalized toroidal beta) is above the Troyon limit. For the above two reasons, this part of the curve is plotted with a dashed line and will not be discussed below. We see that the confinement capability is maximum for a point called marginally sustained ignition (MSI) because it is the last surviving operating point when the confinement time is decreased with respect to the value given by the scaling law. MSI is obtained for $\langle T \rangle_n \simeq 7.8$ keV in both machines. We see that the ignition margin is approximately 6% lower in ITER ID than it was in ITER OD.

4.2 ITER ID versus ITER CDA

The comparison between ITER ID and ITER CDA is shown in Fig. 3. MSI ignition is also obtained for $\langle T \rangle_n \simeq$7.8 keV in ITER CDA. We see that the maximum ignition margin is 5% less in ITER ID than it was in ITER CDA. However, extrapolation in the elongation dependance of the confinement time is made for ITER CDA up to values which are outside the database.

5 Effect of τ^*_{He}/τ_E for ignition in ITER ID

The ignition curves for P_{fus}=1500 MW are plotted in Fig. 4 for τ^*_{He}/τ_E=5, 10, 12, 15, 17.5. We see that increasing the apparent helium confinement time both reduces the operating range and increases the available operating densities. For $\tau^*_{He}/\tau_E \geq 17.6$, the ignition curve no longer exists.

Values of the confinement capabilities are given in Fig. 5 for τ^*_{He}/τ_E=5, 10, 15. The ignition margin at MSI gains 12 % when τ^*_{He}/τ_E decreases from 10 to 5; it losses 22 % when τ^*_{He}/τ_E increases from 10 to 15.

6 Operation in driven mode

Constant P_{fus}, P_{ext} curves are plotted in Fig. 6 for P_{ext}=0, 50, 100 MW. We see that operation in driven mode with increasing external power both widens the operation temperature range and allows operation at lower densities.

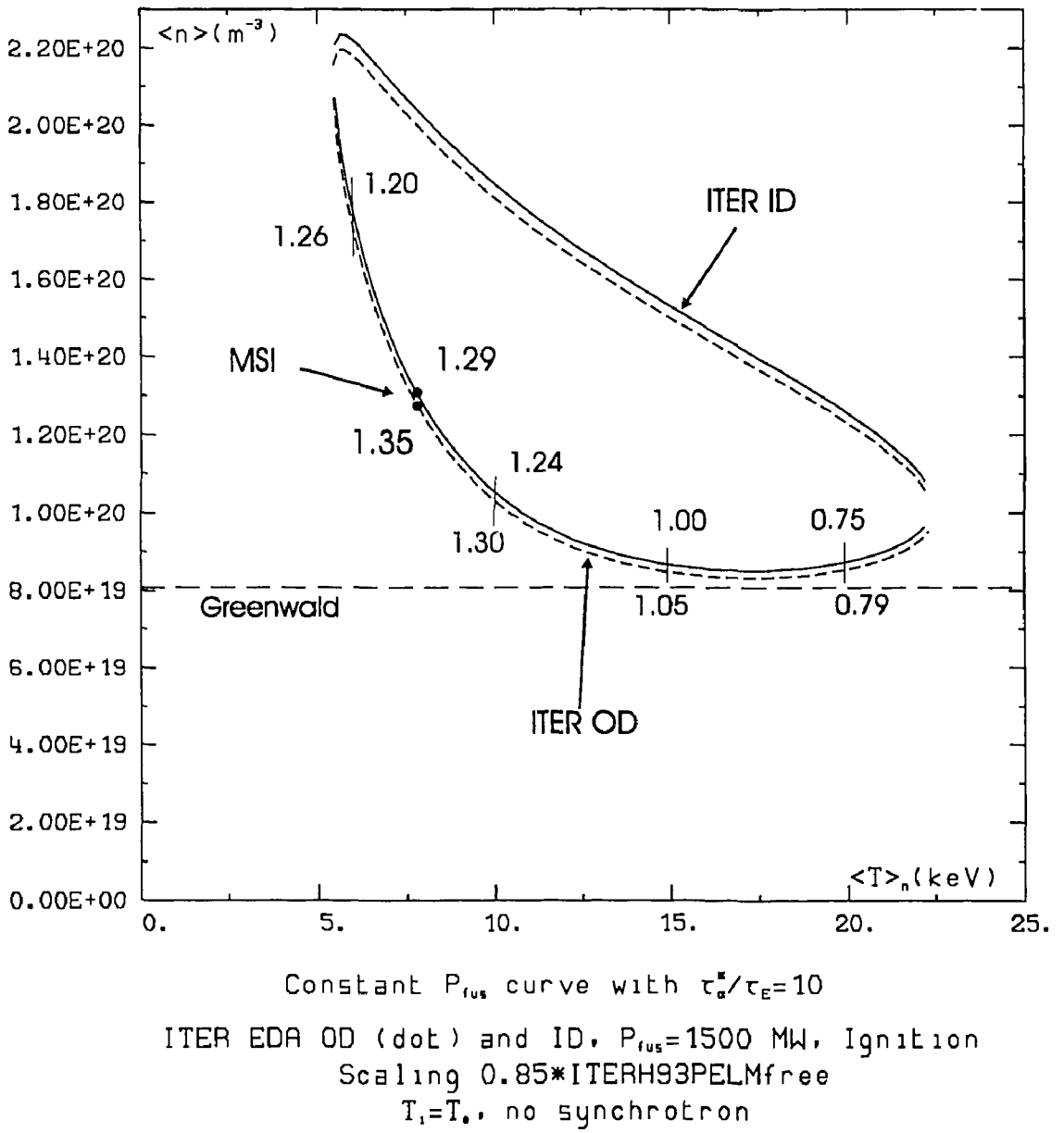

Figure 2: Comparison of ignition margins in ITER OD and ITER ID, P_{fus}=1500 MW, τ^*_{He}/τ_E=10. The numbers which label the operating points are the confinement capabilities M.

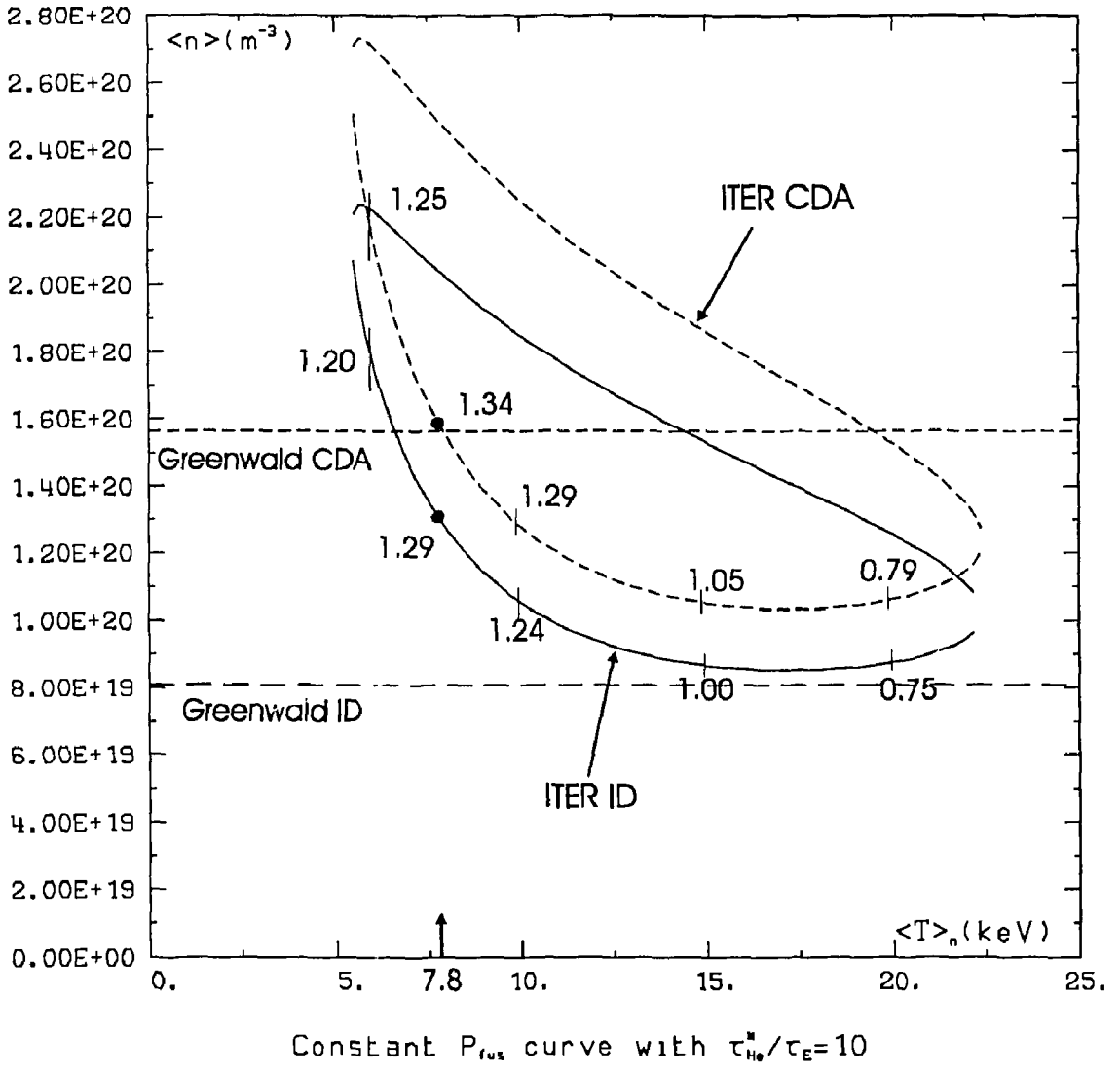

Constant P_{fus} curve with τ^*_{He}/τ_E=10

ITER CDA (dot): P_{fus}=1100 MW and EDA ID: P_{fus}=1500 MW
Ignition, Scaling 0.85*ITERH-93P-ELM-free
$T_i=T_e$, no synchrotron

Figure 3: Comparison of ignition margins in ITER CDA (P_{fus}=1100 MW) and ITER ID (P_{fus}=1500 MW) for τ^*_{He}/τ_E=10.

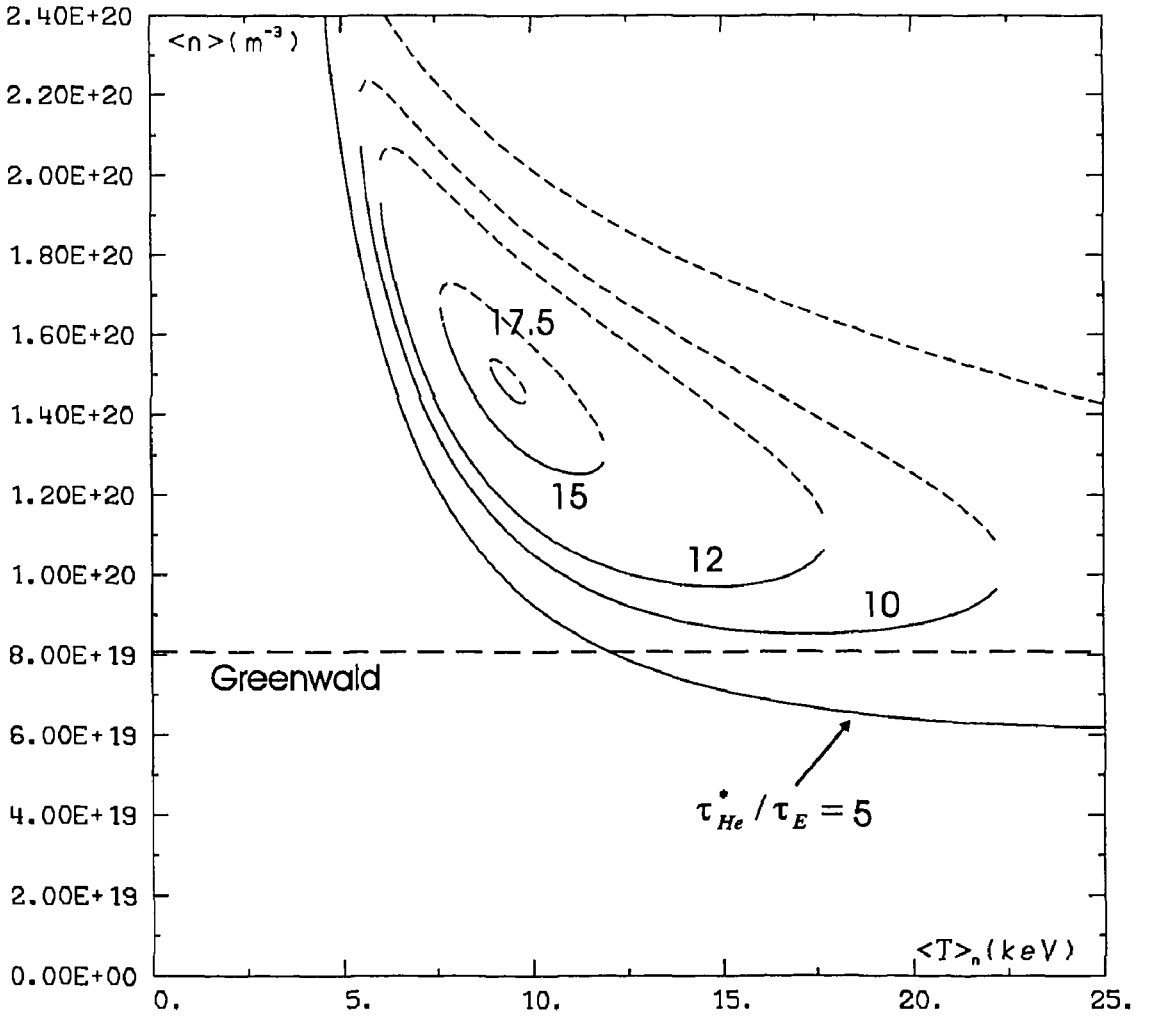

Figure 4: ITER ID ignition curves for P_{fus}=1500 MW and τ^*_{He}/τ_E=5, 10, 12, 15, 17.5.

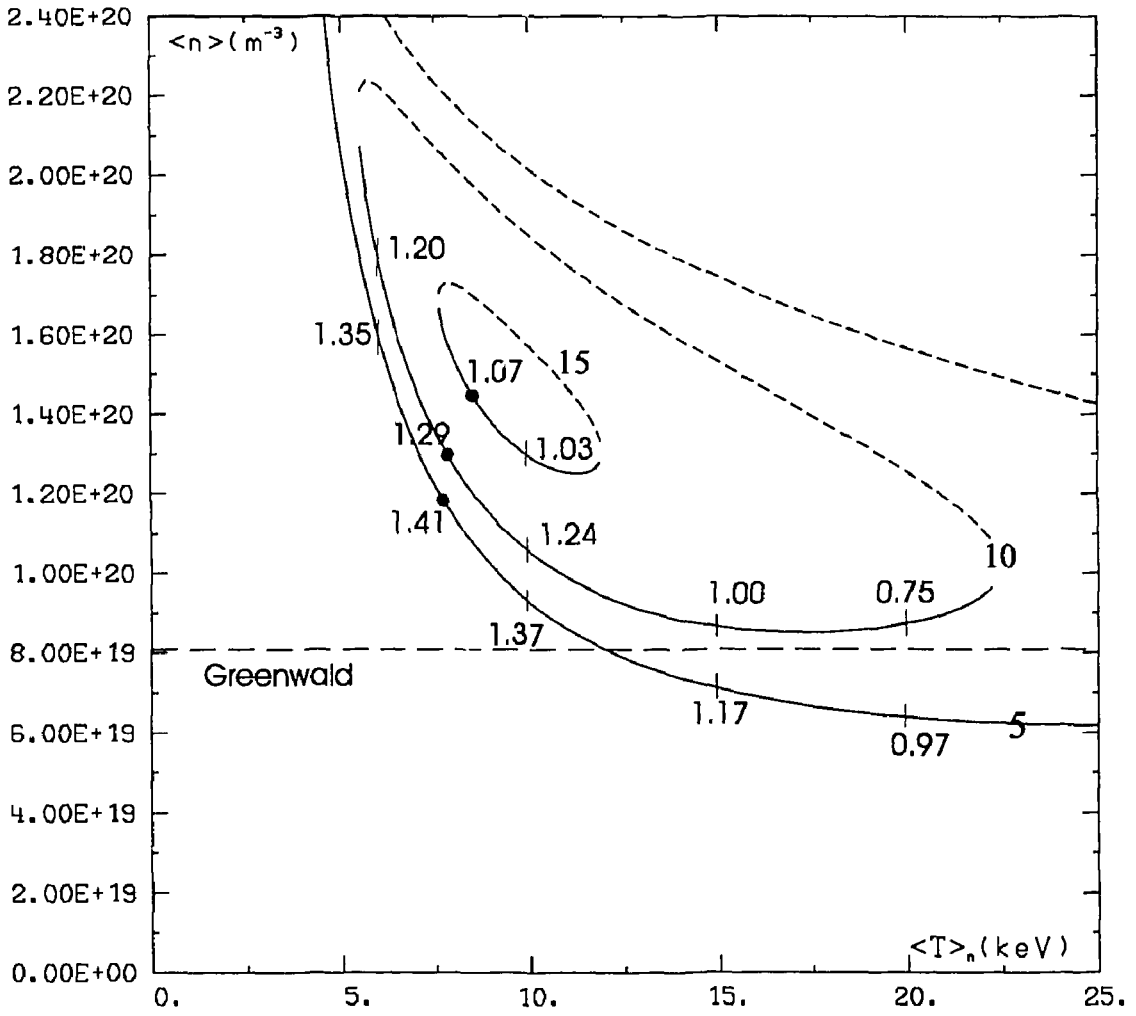

Figure 5: ITER ID ignition curves for P_{fus}=1500 MW and τ^*_{He}/τ_E=5, 10, 15.

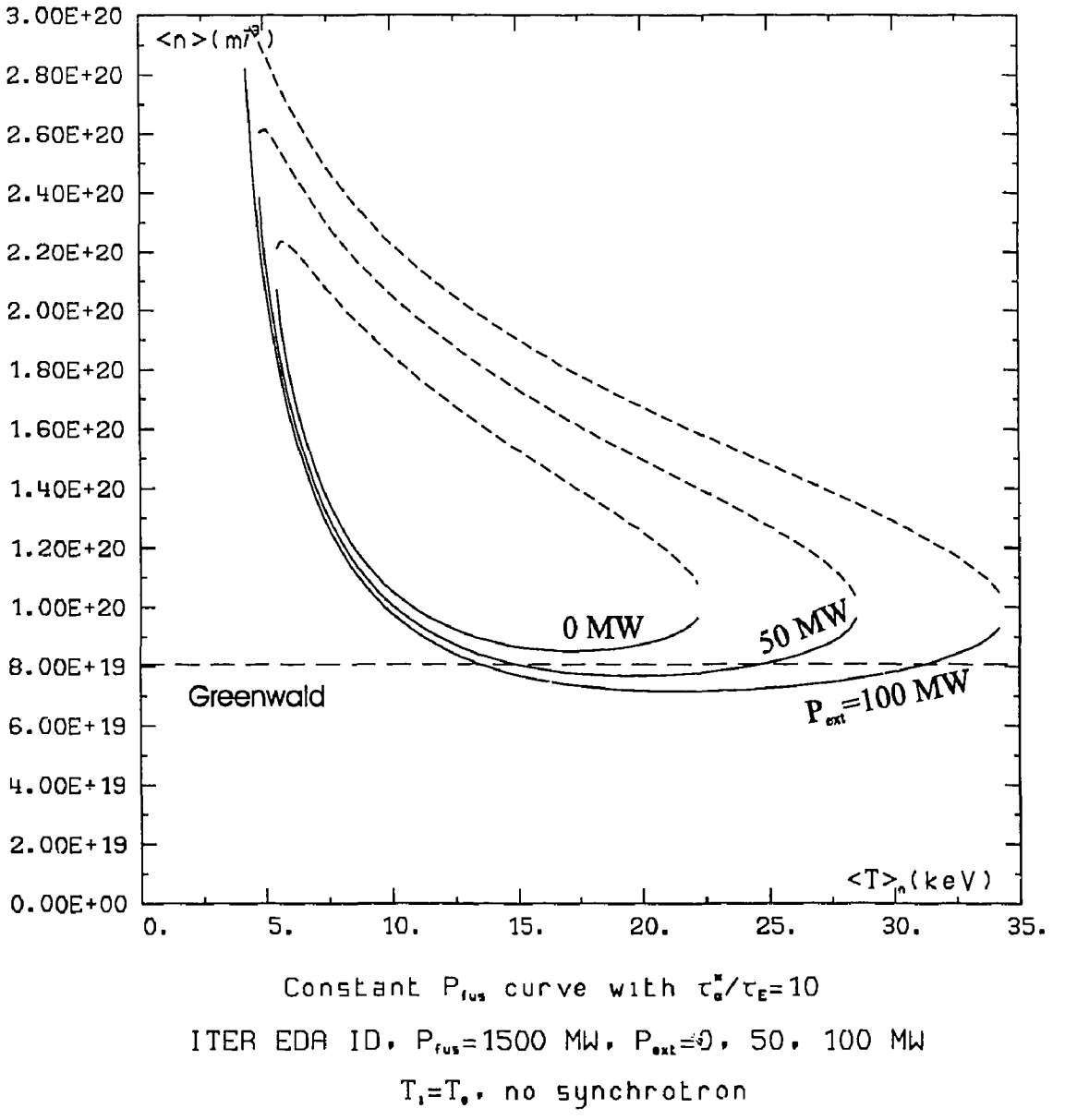

Figure 6: ITER ID constant P_{ext} curves for P_{fus}=1500 MW, τ^*_{He}/τ_E=10 and P_{ext}=0, 50, 100 MW.

Values of the confinement capabilities are given in Fig. 7 for τ_{He}^*/τ_E=10 and P_{ext}=50, 100 MW. Marginally sustained thermal equilibrium (MSE) is obtained for $\langle T \rangle_n \simeq 7.5$ keV in both cases. For P_{ext}=50 MW, the confinement margin at MSE is 42 % (+ 13 % with respect to the pure ignition case). For P_{ext}=100 MW, the confinement margin at MSE is 53 % (+ 24 % with respect to the pure ignition case).

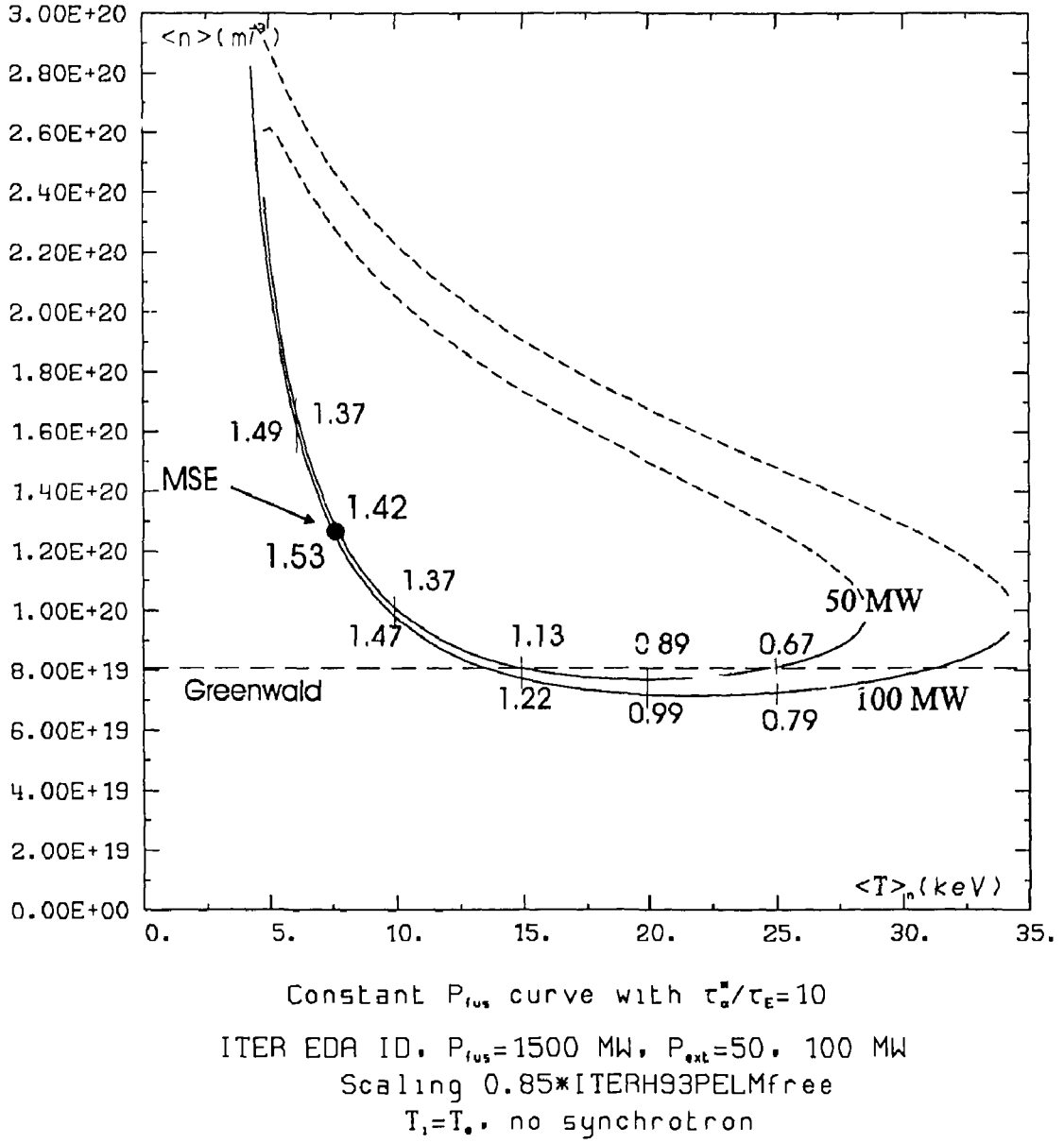

Figure 7: ITER ID constant P_{ext} curves for P_{fus}=1500 MW, τ_{He}^*/τ_E=10, and P_{ext}=50, 100 MW.

7 Effect of the fusion power

The ITER ID ignition curves are plotted in Fig. 8 for τ_{He}^*/τ_E=10 and P_{fus}=1500 MW (corresponding to $\Gamma_n \simeq 0.96$ MW/m^2) and 1000 MW ($\Gamma_n \simeq 0.64$ MW/m^2). Values of the confinement capabilities M are also given. We see that the ignition margin at MSI is slightly better at lower fusion power and that a range of operating points below the Greenwald density limit is now available.

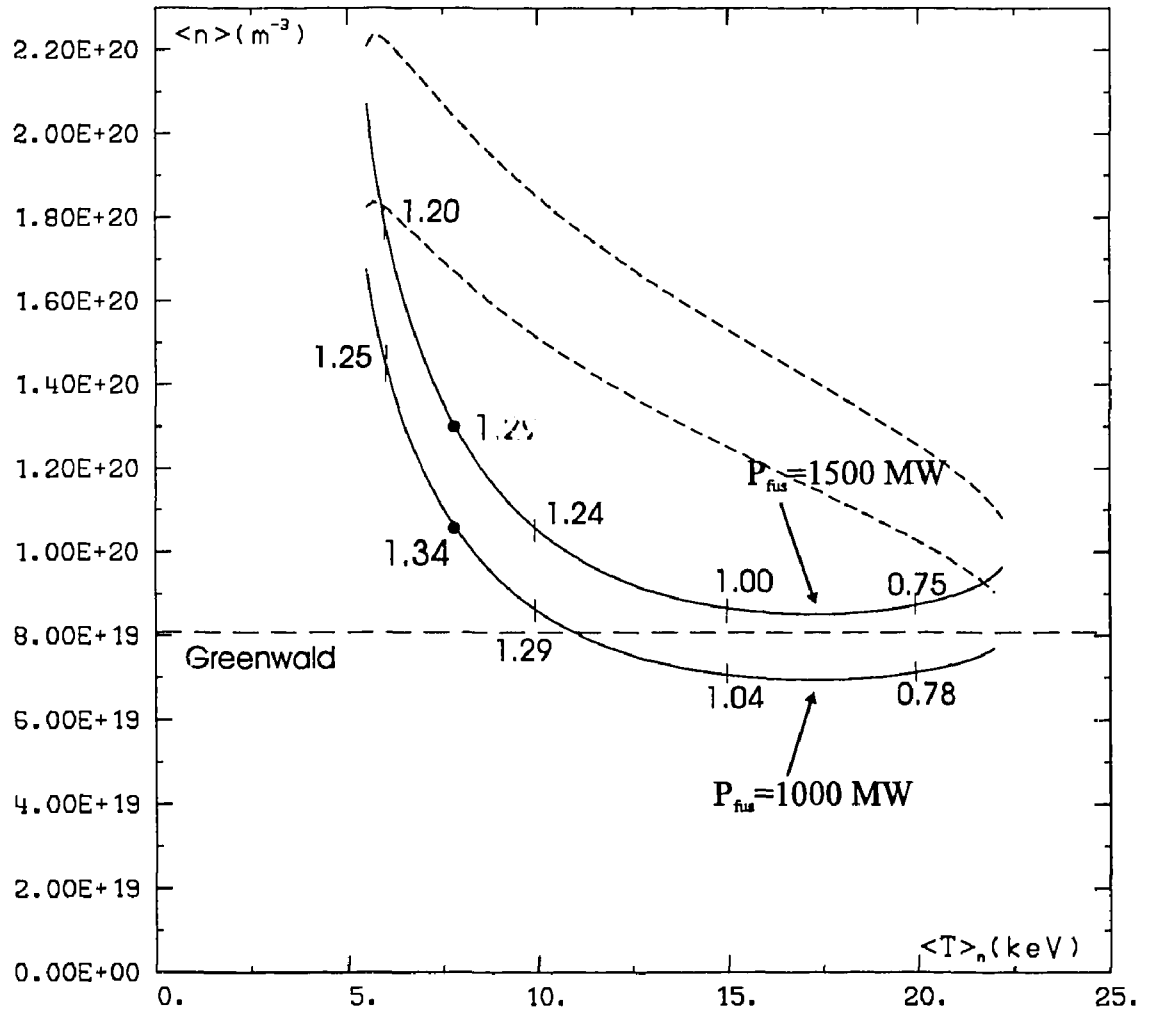

Constant P_{fus} curve with τ_α^*/τ_E=10

ITER EDA ID, P_{fus}=1500 MW, 1000 MW, ignition
Scaling 0.85*ITERH93PELMfree
T_i=T_e, no synchrotron

Figure 8: ITER ID ignition curves for τ_{He}^*/τ_E=10 and P_{fus}=1500 MW and 1000 MW.

8 Effect of the toroidal magnetic field intensity

The risk not being able to obtain the reference toroidal magnetic field must be taken into account. Here, we look at the consequence on the ignition margin of a reduction of the magnetic field intensity.

In Fig. 9, we have plotted the ignition curves corresponding to the reference magnetic field and to 10% and 20% reductions in both the magnetic field and the plasma current (in order to work at constant $q_{\psi 95}$). We see that the (n, T) plots are practically identical for the three cases. The slight shift between the curves is due to the variation of the ohmic power. For a 10% reduction, the maximum ignition margin reduces to 11% (-18% relatively to the nominal value). For a 20% reduction, the ignition margin becomes negative (-5%) representing a 34% loss with respect to the nominal case.

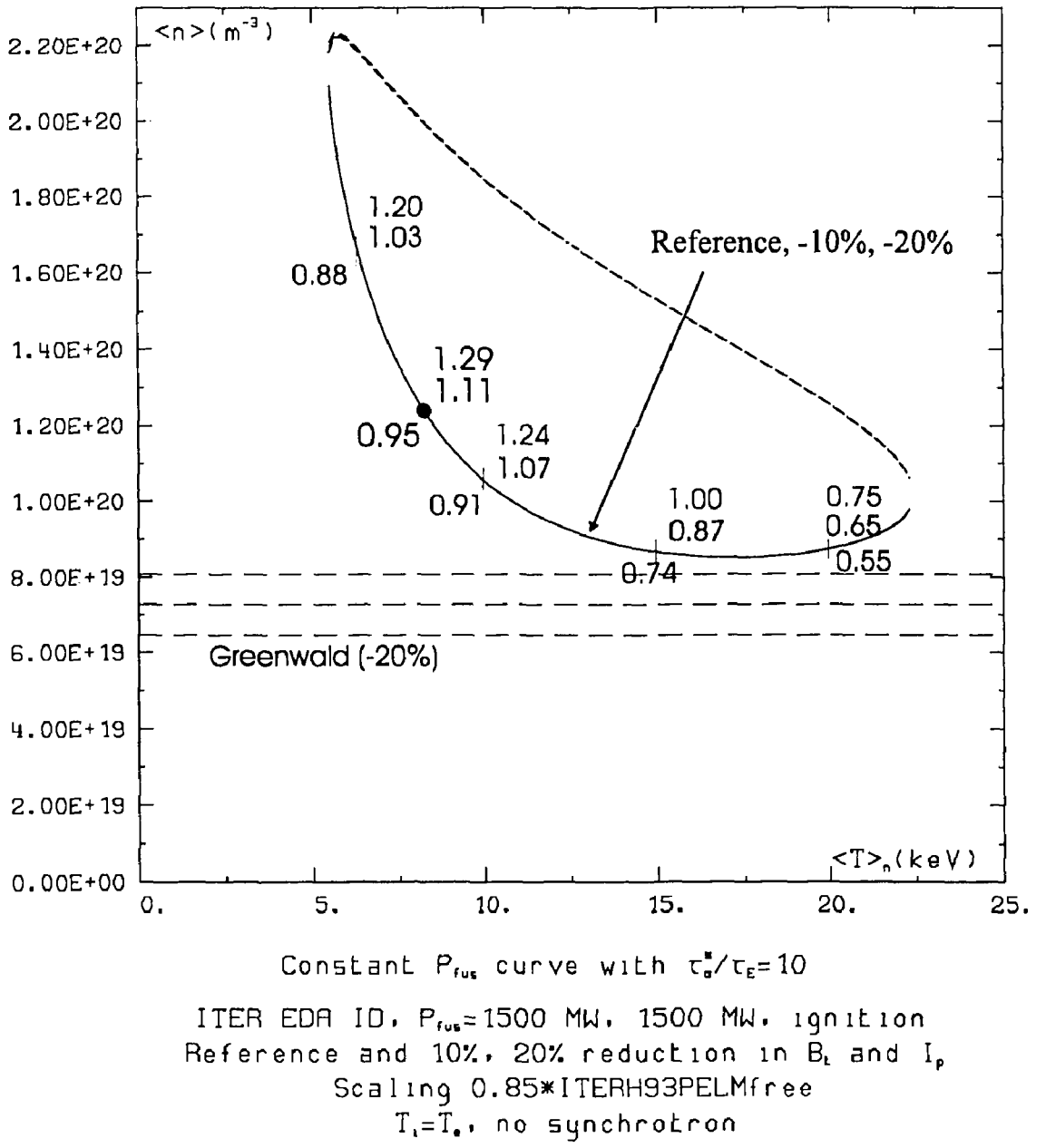

Figure 9: ITER ID ignition curves for τ^*_{He}/τ_E=10, P_{fus}=1500 MW, for the reference B_t, I_p and for a 10% and 20% reduction of these parameters.

9 Effect of the neon contents

Neon is envisaged in ITER as a seed impurity to obtain detached radiative divertor H-mode plasmas. In Fig. 10, we have represented the P_{fus}=1500 MW, τ^*_{He}/τ_E=10 ignition curves with fraction of neon in the main plasma f_{Ne}=0%, 0.68% and 0.75%. We see that the ignition margin is reduce to zero when f_{Ne}=0.68%. For f_{Ne}=0.76%, the ignition curve no longer exists.

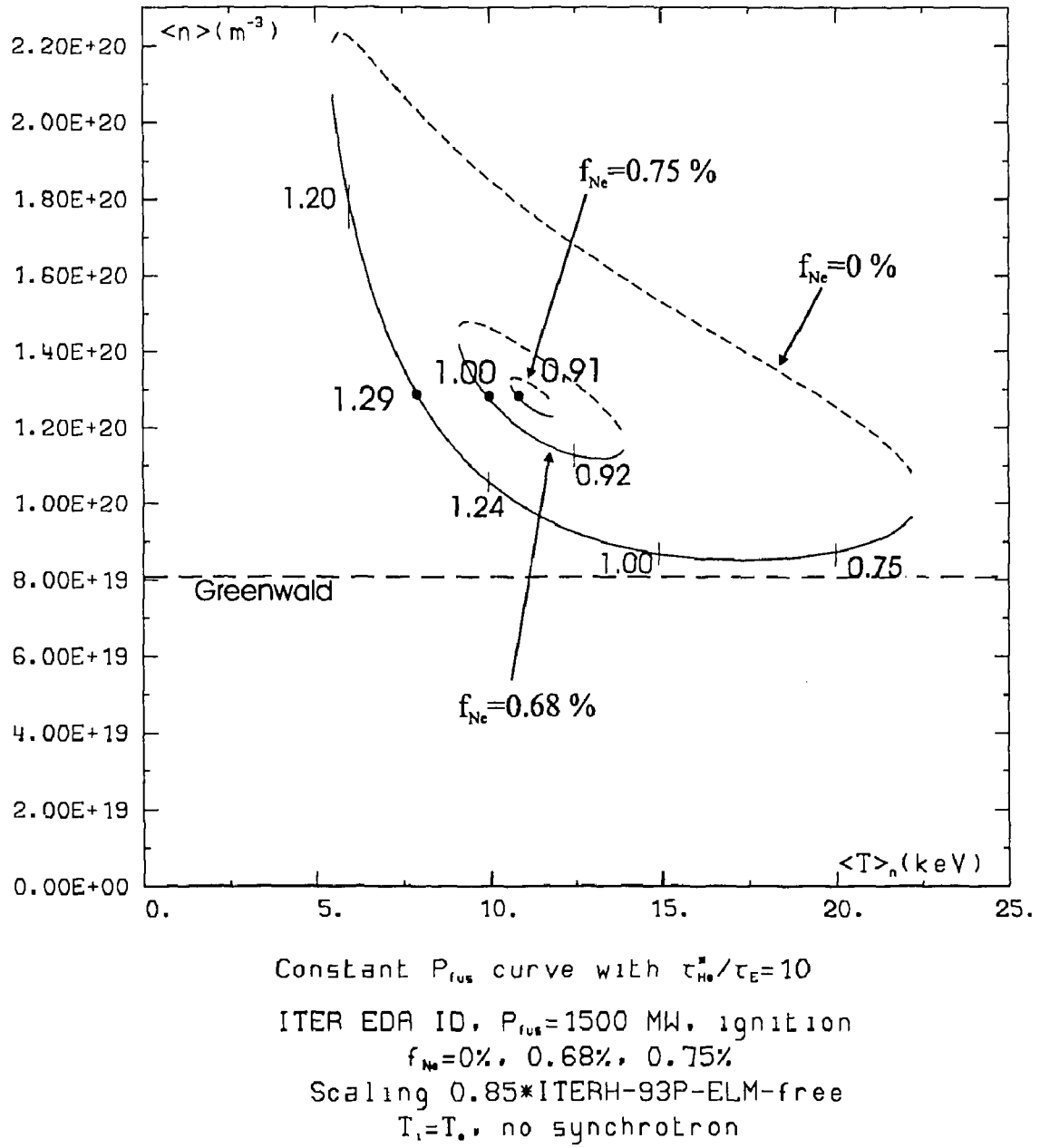

Figure 10: Effect of neon contamination on the ignition curves and ignition margins.

10 Conclusions

The above calculations have been performed without taking the small volume variation due to the lower X-point into account. The calculated ignition margins are then slightly overestimated. Inclusion of the correct geometry is in progress.

The calculations underline the great sensitivity of the ignition margin with respect to the helium content (dilution effect). However, we have found that ignition is still possible for τ_{He}^{*}/τ_E values as high as 15 provided averaged densities of about $1.3\times10^{20}\mathrm{m}^{-3}$ can be achieved.

Operation in driven mode with Q=30 (P_{ext}=50 MW) or Q=15 (P_{ext}=100 MW) considerably increases the confinement capability if proper operation of the divertor may be achieved.

Downgrading the fusion power output could allow operation at densities below the Greenwald limit at the expense of a reduction of the neutron flux.

Realizing the nominal magnetic field is essential. Lowering the field both considerably reduces the ignition margin and causes a downward shift of the Greenwald density limit with respect to the available operating densities.

Finally, we have seen that main plasma contamination by neon would prevent ignition for neon fractions as low as 0.7%.

References

[1] J. JOHNER, EUR-CEA-FC-1429 report, October 1991.

[2] H-MODE DATABASE WORKING GROUP, presented by D.P. SCHISSEL, 20th EPS Conf. on Controlled Fusion and Plasma Physics 1993 (Lisbon), Vol. 17c, part I, p. 103.

List of Figures